Materials Characterization 200 (2023) 112863

Contents lists available at ScienceDirect

Materials Characterization

journal homepage: www.elsevier.com/locate/matchar

Investigation on the novel copper-based composite conductors synergistically improved by in-situ generated graphene and nanoparticles

Tingting Zuo [a], Meng Wang [a], Jiangli Xue [a], Yadong Ru [a], Yue Wu [a], Fazhu Ding [a,b], Bo Da [c], Zhuang Xu [a], Peter K. Liaw [d], Zhaoshun Gao [a,b,*], Li Han [a,b], Liye Xiao [a,b]

[a] Institute of Electrical Engineering Chinese Academy of Sciences, Beijing 100190, China
[b] University of Chinese Academy of Sciences, Beijing 100049, China
[c] Research and Services Division of Materials Data and Integrated System, National Institute for Materials Science, Tsukuba 305-0047, Japan
[d] Department of Materials Science and Engineering, The University of Tennessee, Knoxville, TN 37996, USA

ARTICLE INFO

Keywords:
Metal-matrix composites
Graphene
Mechanical properties
Microstructure
Nanoparticle

ABSTRACT

High-performance Cu/graphene composites synergistically strengthened by nanoparticles were directly synthesized by hot press sintering using different organometallic substances, such as aluminum stearate, zinc stearate, and tetrabutyl titanate, as the graphene and nanoparticle formation source. The TiO_2-doped Cu/Graphene composite possesses high hardness, great plasticity, and high electrical conductivity due to the uniformly-distributed three-dimensional (3D) network graphene and the TiO_2 nanoparticles at the Cu/graphene interface. The composite wire processed by severe cold deformation without intermediate heat treatment displays high electrical conductivity of 92.3% IACS, great tensile strength of 497 MPa, and high softening temperature close to 400 °C, for which the graphene hinders the grain boundary movement and pins the dislocations, the TiO_2 nanoparticles nail the interface and increase the roughness of graphene, the fibrous grains and the thinned graphene along the grain boundary provide a fast path for electron transmission. The present work offers a novel pathway for designing and fabricating high-performance Cu/Graphene conductors.

1. Introduction

The demand for high strength and great conductivity of copper alloys continues to increase with the advancement of technology in modern electric power systems, aerospace and transportation industries, and advanced electronic and communication devices [1,2]. However, due to the intrinsic physical characteristics of copper and the limitations of traditional strengthening methods of copper alloys [3,4], it is still hard to simultaneously obtain high strength and great conductivity. Developing new materials to further improve the combination of strength and conductivity is urgently needed. A copper/carbon composite is a promising alternative to conventional Cu due to its improved current-carrying capability and enhanced mechanical strength [5–11]. Among all, graphene consisted of sp^2-hybridized carbon atoms with excellent electrical, thermal, and mechanical properties, is reckoned as the ideal reinforcement material for copper alloys [12–14]. Till now, so much attention has been put into this area and a great number of works have been reported on the fabrication and properties of graphene reinforced copper matrix composites [15–20]. However, due to the difficulty in dispersing graphene in the copper, the performance of Cu/Gr composites is far from meeting the designed value. Different methods, such as ball milling [15], electrochemical deposition [16], chemical reaction [19,21], and chemical vapor deposition (CVD) [22], are applied to solve the above problem. Ball milling [9] as the most commonly used method, facilitates the dispersion of graphene but is easy to introduce defects and impurities. Electrochemical deposition [16] can achieve uniform dispersion of Gr, but it is not easy to prepare bulk samples with Cu/Gr films. Chemical reaction [5] often uses graphene oxides to synthesize composites that can realize the uniform dispersion, but the whole process is too complicated. By contrast, CVD solves graphene agglomeration by in-situ grown graphene on copper powders [17]. But due to the intrinsic character of Gr and Cu powders, the interface connectivity still needs to be further improved. Besides, the three-dimensional (3D) structured graphene by in-situ preparation existing at the grain boundary mainly achieves the effect of grain refinement strengthening by limiting grain growth [18]. Exploiting two or more phases to synergistically enhance the metal matrix by different strengthening mechanisms provides superior performance compared to using only a single

* Corresponding author at: Institute of Electrical Engineering, Chinese Academy of Sciences, Beijing 100190, China.
E-mail address: gaozs@mail.iee.ac.cn (Z. Gao).

https://doi.org/10.1016/j.matchar.2023.112863
Received 1 February 2023; Received in revised form 13 March 2023; Accepted 28 March 2023
Available online 2 April 2023

reinforcement phase composite [23,24]. For example, Xu et al. [23] developed an in-situ solid-state reaction method to incorporate graphene nanosheets and WC_{1-x} nanoparticles into a copper matrix to achieve synergistic strengthening and toughening effects. Shi et al. [25] have proposed an idea of introducing Al_2O_3 particles to adjust the surface roughness of graphene to not only optimize the interfacial bonding but also increase the strength, which brings about a new insight.

Here, in order to simultaneously solve the dispersion of Gr, the weak bonding between the Gr and Cu matrix, and introduce more enhancement phases to synergistically strengthen the metal matrix, organometallic compounds are selected as the carbon source to in-situ introduce Gr and nanoparticles during hot press sintering, which arouse the composites to show simultaneous high strength and great electrical conductivity. The synergetic effect strategy in our work might offer a novel pathway for designing high-performance Cu/Graphene conductors.

2. Material and methods

2.1. Fabrication of Gu/Gr composite

Spherical Cu powder with a purity of 99.9 wt% (wt%) and particle sizes smaller than 20 μm and different kinds of organometallic compounds such as aluminum stearate ($C_{36}H_{71}AlO_5$), zinc stearate ($C_{36}H_{70}ZnO_4$), magnesium stearate ($C_{36}H_{70}MgO_4$), calcium stearate ($C_{36}H_{70}CaO_4$) and tetrabutyl titanate ($C_{16}H_{36}O_4Ti$) were used. Firstly, 15 g Cu powders were mixed with different qualities of organometallic compounds by mechanical grinding. The mass of the organometallic compound is 0.1352 g, 0.1223 g, 0.9891 g, 0.1023 g and 0.0503 g for aluminum stearate, zinc stearate, magnesium stearate, calcium stearate, and tetrabutyl titanate, respectively, which is calculated according to that the metal element is completely converted into oxides and the volume percentage of the oxides is 0.5%. Secondly, the mixed powders were put into a Φ12.7 mm graphite die and hot-pressed at a pressure of 50 MPa and 900 °C for 1 h in a high vacuum (5×10^{-3} Pa). Then the polished sintered sample with the dimension of Φ12.4 mm was cold forged into Φ8 mm rods, cold rolled to Φ3.2 mm, and then cold drawn to 0.49 mm. Finally, the cold drawn wires were annealed at different temperatures for 1 h in a high vacuum. For comparison, pure Cu samples were prepared by the same process. For simplicity, these composites doped with aluminum stearate, magnesium stearate, zinc stearate, calcium stearate, and tetrabutyl titanate are referred to as Cu/Gr-Al, Cu/Gr-Mg, Cu/Gr-Zn, Cu/Gr-Ca, and Cu/Gr-Ti, respectively. The schematic diagram of the preparation process of the samples is shown in Fig. 1.

2.2. Microstructure characterization and performance testing

The crystal structures of the composites were identified by an X-ray diffractometer (XRD) under Cu Kα radiation, with a scanning speed of 10°/min and a step size of about 0.02°. The microstructures of the samples were characterized by scanning electron microscopy (SEM, ZEISS SIGMA), electron backscattered diffraction (EBSD), and transmission electron microscopy (TEM, JOEL 2100) with energy dispersive spectrometry (EDS). The structural defects of the in-situ formed Gr were analyzed by Raman spectroscopy (RENISHAW inVia), using a 532 nm green diode laser. The X-ray photoelectron spectroscopic (XPS) measurements were carried out on a PHI Quantera II system to analyze the element and valence of the composites. The carbon content of the samples was obtained by the high-frequency infrared carbon and sulfur analyzer (2021CS-901B). The amount of metal elements actually doped was detected by wavelength dispersive X-ray fluorescence spectrometer (ZSX Pimus II). The tensile properties of the cold drawn wires with a gage length of 50 mm, and a diameter of 0.49 mm were conducted on a CMT6104 universal machine from MTS at the tensile rate of about 0.5 mm/min. The hardness of deformed and annealed samples was measured at 9 points by the sclerometer with a load of 200 g and a holding time of 15 s. By removing the maximum and minimum values, the average hardness was got from the remaining 7 points. The electrical conductivity of bulk and sheet samples was measured by the Sigma 2008B eddy current conductivity meter at three different places on both sides, the electrical conductivity of the composite wires was measured by the high-precision Keithley current-voltmeter (cold drawn wires) at ambient temperature for three samples on the same wire, then the average value was got.

3. Results and discussion

3.1. The microstructure of graphene and nanoparticles synergistically strengthened Cu composite and its formation process

A previously reported in-situ preparation method was used to grow graphene inside the Cu matrix [18,26]. A large difference here is the different organometallic compounds used as the carbon source. The SEM images in Fig. 2(a) and (b) give the typical two-phase structure of the sintered composite using the aluminum stearate as the carbon source (Cu/Gr-Al), for which the dark area is the Cu matrix, the bright area is the graphene, and graphene mostly exist along the grain boundary. After etching the copper matrix in the mixed $FeCl_3$ and HCl solution, the 3D discontinuous network structure of graphene is clearly seen [Fig. 2(c)].

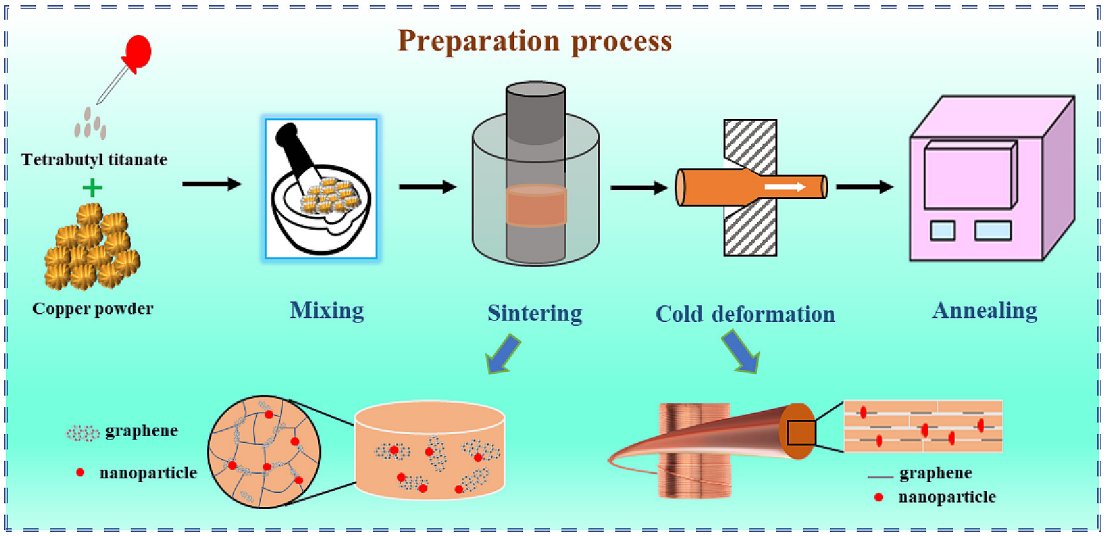

Fig. 1. The schematic diagram of the sample preparation process.

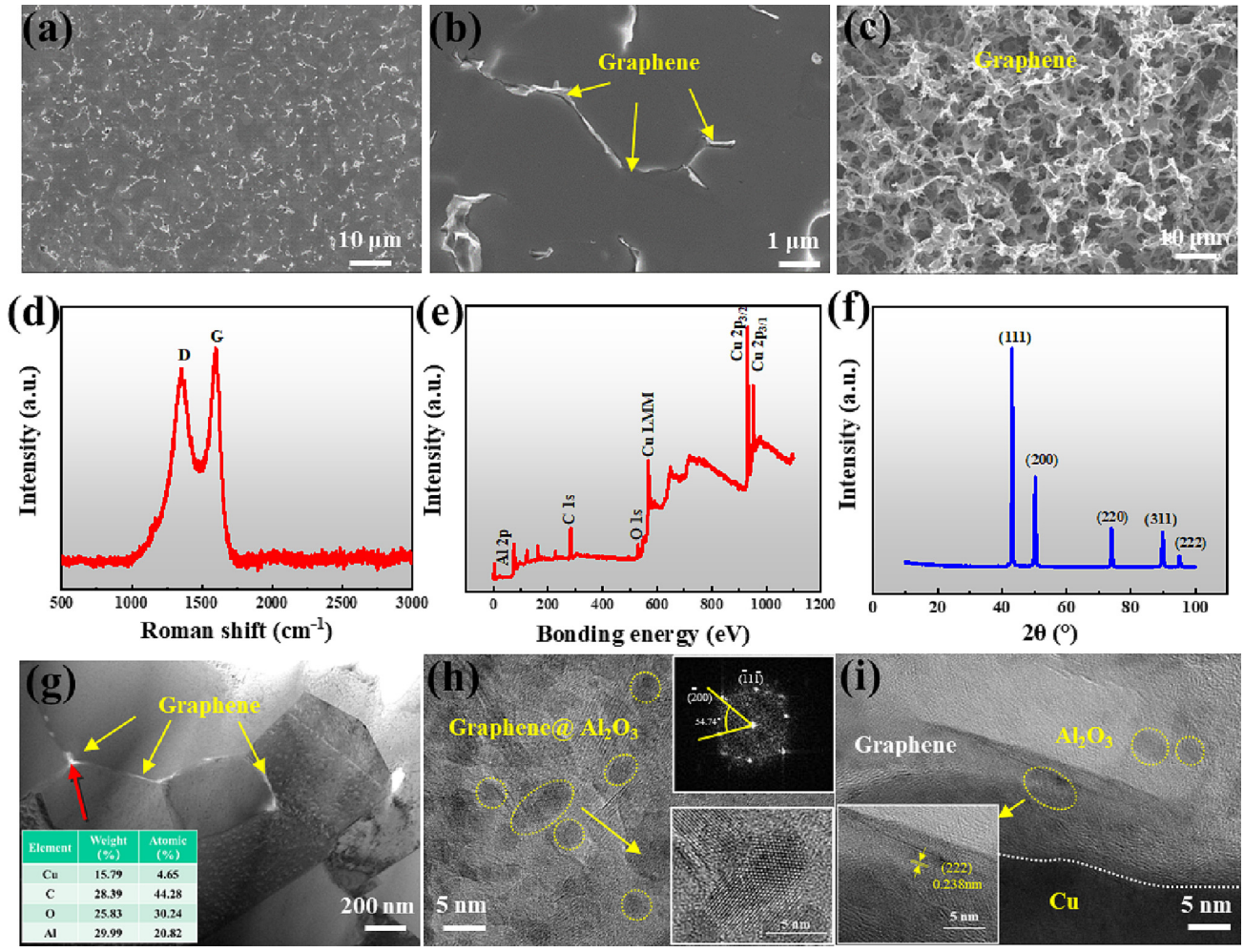

Fig. 2. The microstructure of the Cu/Gr-Al composite (a) and (b) SEM images; (c) the 3D Gr skeleton of the composite etched by the mixed $FeCl_3$ and HCl solution; (d) the Raman spectrum of the Gr; (h) XPS spectra and (f) the XRD pattern of the sintered Cu/Gr-Al composite; (g) TEM bright field image; (h) and (i) the HRTEM images of the interface and graphene area.

The Raman spectroscopy in Fig. 2(d) with the D/G ratio of about 0.87 confirms that the resulting graphene is defective and multi-layered, for which the 2D peak is disappeared. This may stem from the irregular surface of the copper powder, the high concentration of carbon source, and the long growth process without H_2 [27,28]. The XPS spectroscopy measured shows O1s (531 eV), Cu LMM (570 eV), Cu 2p3/2 (931 eV), Cu 2p1/2 peak (952 eV), and Al 2p peak (74.8 eV). However, by the EDS measurement, the Al element is not found which implies a very little amount of Al. To validate the purpose of the design, the TEM experiment was conducted, and the bright-field TEM microstructure in Fig. 2(g) is similar to that of SEM. The local EDS result shows that Al is rich in the graphene area. From the HRTEM image in Fig. 2(h) and (i), a great number of nanoparticles are found at the Gr area and Cu/Gr interface. By calibrating the interplanar spacing and the diffraction pattern of the yellow area and combining with the atomic percentage of Al to C, it is determined that the nanoparticles are γ-Al_2O_3 particles. From Fig. 2(i), there is an evident transition zone between the Gr and Cu matrix, without voids and impurities, which implies a strong interface. From the above results, it is deduced that during the sintering process, the aluminum stearate decomposes into Al_2O_3 and carbon groups, and then the carbon groups grow into graphene under the catalysis of copper at a high temperature.

3.2. *The microstructure and performance of Cu/Gr composites fabricated by different carbon sources*

Based on the above design, different organometallic compounds have been selected as the carbon sources to explore their effects on the properties of the composites. Fig. 3 shows the variation trend of electrical conductivity and hardness using different carbon sources. It is clear that the hardness increases substantially by doping all carbon sources compared with pure copper. Besides, compared with the graphene reinforced copper composites with high carbon content prepared by using liquid paraffin as the carbon source in our previous work, the hardness is significantly higher, which is not only due to the graphene, but also be attributed to the strengthening effect of nano oxide particles [18]. However, the electrical conductivity all decreases. By comparison, the Cu/Gr-Al and Cu/Gr-Ti composites possess both high hardness and great electrical conductivity, for which the hardness values are 75.8 HV and 79.3 HV and the electrical conductivity values are about 92.1 % IACS and 95.2 %IACS, respectively.

In order to explore the factors influencing the properties, the microstructures are analyzed, as exhibited in Fig. 4. All composites present multiple phases with the dark Cu matrix and bright Gr phase. The typical D band representing defects at 1368 cm^{-1} and the G band denoting crystallinity at 1576 cm^{-1} confirm the existence of the multi-layer Gr. The intensity ratio between the D and G bands (I_D/I_G = 0.76– 0.90) implies the relatively high defects of the formed Gr [29]. The obvious

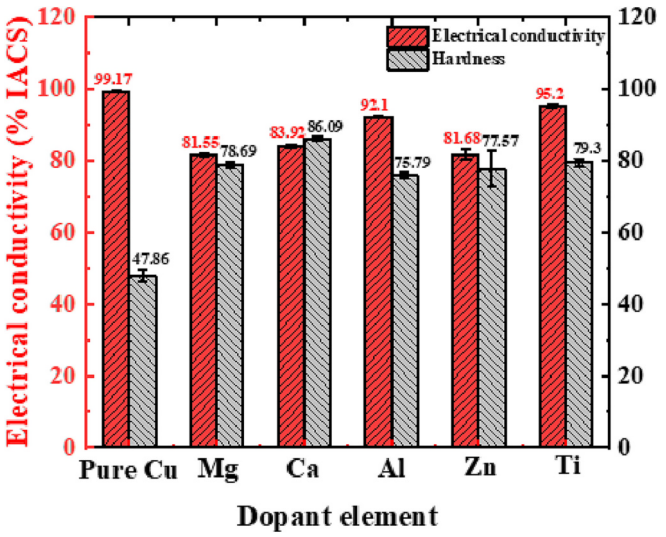

Fig. 3. The variation trend of electrical conductivity and hardness by introducing different carbon sources.

peak at 611 cm^{-1} in Fig. 4(l) should be from TiO_2 according to the literatures [30,31] After etching, the three-dimensional (3D) network morphology of graphene for all samples is clearly seen, especially the Cu/Gr-Al composite [Fig. 2(c)]. The carbon content of these composites which can be related to the doping content of the organometallic compounds is 0.1266 wt%, 0.073 wt%, 0.1509 wt%, 0.1602 wt%, and 0.052 wt% for Cu/Gr-Al, Cu/Gr-Mg, Cu/Gr-Zn, Cu/Gr-Ca, and Cu/Gr-Ti, respectively. Since the in-situ grown graphene is flawed and relatively thick, it makes the electrical conductivity decrease. But compared with Cu/Gr composites prepared by other methods, the conductivity reduction of this in-situ graphene strengthened Cu composite is relatively small [15,32]. By consideration of the properties and microstructure, it indicates that the less content, the thinner, and the better the quality of Gr with 3D structure, the higher the electrical conductivity and the hardness [33,34], especially the Cu/Gr-Ti composite. Besides, other factors, such as the microstructure of the matrix, the interface bonding condition, and the content and properties of the oxide, can also influence the overall performance [18,35].

Since it is difficult to detect oxide nanoparticles from the SEM image and EDS analysis, TEM is conducted on the Cu/Gr-Ti sample. Fig. 5(a) provides a TEM image of the sintered Cu/Gr-Ti composite. The polycrystalline structure is clearly visible, with graphene mostly distributed at the grain boundaries. By zooming in on the area where the graphene is located, a large number of nanoparticles are shown on top of the graphene or at the Cu/graphene interface [Fig. 5(b) and (d)]. By the local EDS analysis, these particles are Ti-containing substrates. The HRTEM images of the red rectangle areas in Fig. 5(b) and (d) confirm that this kind of particle is TiO_2, which is well bonded to the Cu matrix and graphene without a clear interface or holes. The size of the particle varies from 5 nm to 50 nm. Thus, it is confirmed that the TiO_2 nanoparticles were in-situ generated during sintering. In particular, the TiO_2 nanoparticles formed at the interface favor pinning the interface and enhancing the interface bonding. In addition, the nanoparticles on top of graphene can increase the surface roughness of graphene and further improve interfacial bonding [25].

However, although Ti doping can effectively improve interfacial bonding, its doping content must be appropriate. Excessive elemental doping can lead to an inhomogeneous structure and deteriorated performance, as seen in Fig. 6. With increasing thecontent of tetrabutyl titanate, the in-situ formed TiO_2 turns to a bulk shape, showing an uneven distribution mostly along the grain boundary, and the graphene becomes thicker and more abundant. All these factors lead to severe scattering of electrons and cause decreased electrical conductivity, without bringing in a noticeable increment of hardness [18].

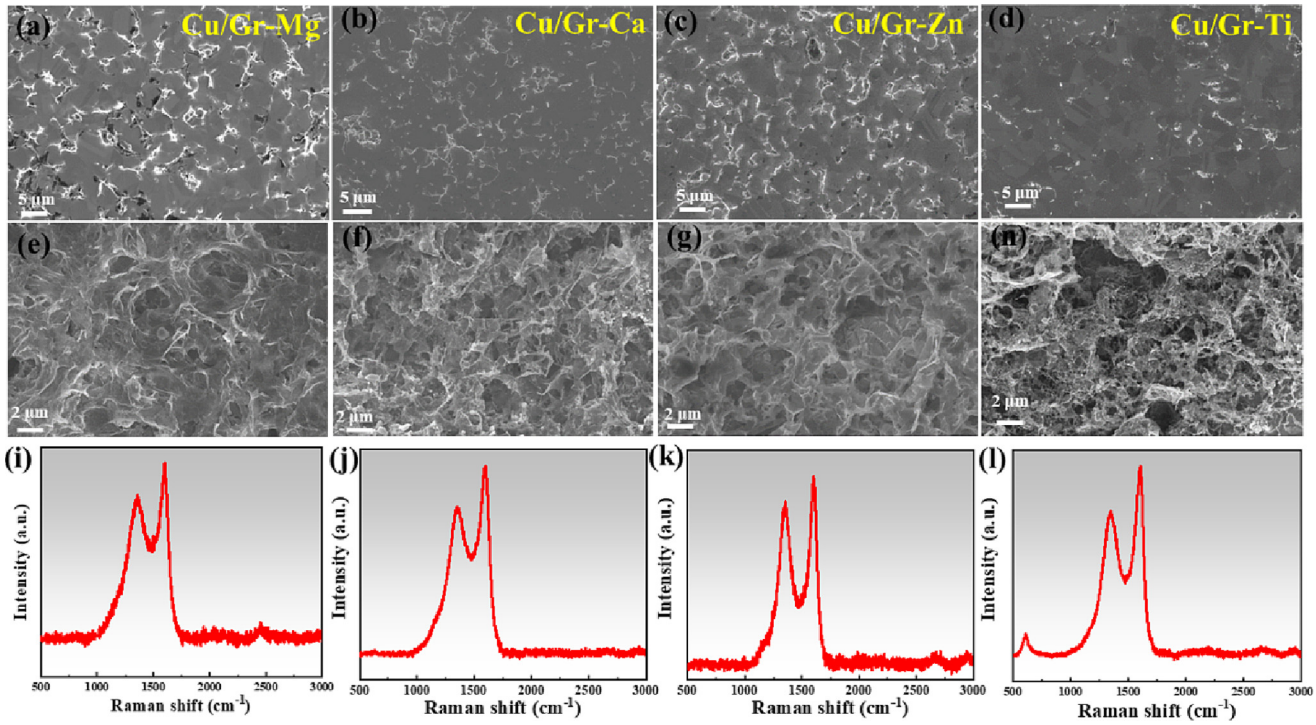

Fig. 4. The SEM images and Raman spectra of sintered Cu/Gr-Mg, Cu/Gr-Zn, Cu/Gr-Ca, and Cu/Gr-Ti composites: (a), (b), (c), and (d) are the SEM images after electrolytic polishing without etching; (e), (f), (g), and (h) are the SEM images after etching in the mixed $FeCl_3$ and HCl solution for 1 h; (i), (j), (k), and (l) are the Raman spectra.

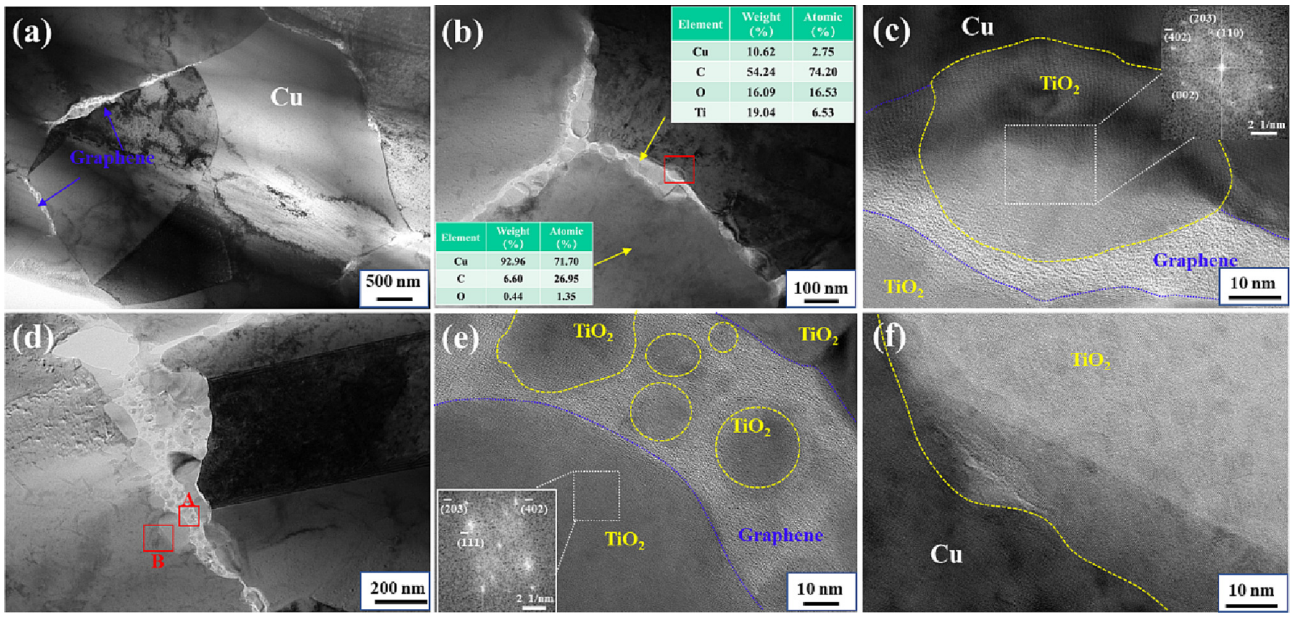

Fig. 5. The TEM image of the sintered Cu/Gr-Ti composite (a), (b) bright-field image, the inset table is the composition of the area indicated by the yellow arrow; (c) the HRTEM image of the red rectangle area in (b); (d) bright-field image; (e), (f) he HRTEM image of the red rectangle area in (d) marked as A and B, respectively. (For interpretation of the references to colour in this figure legend, the reader is referred to the web version of this article.)

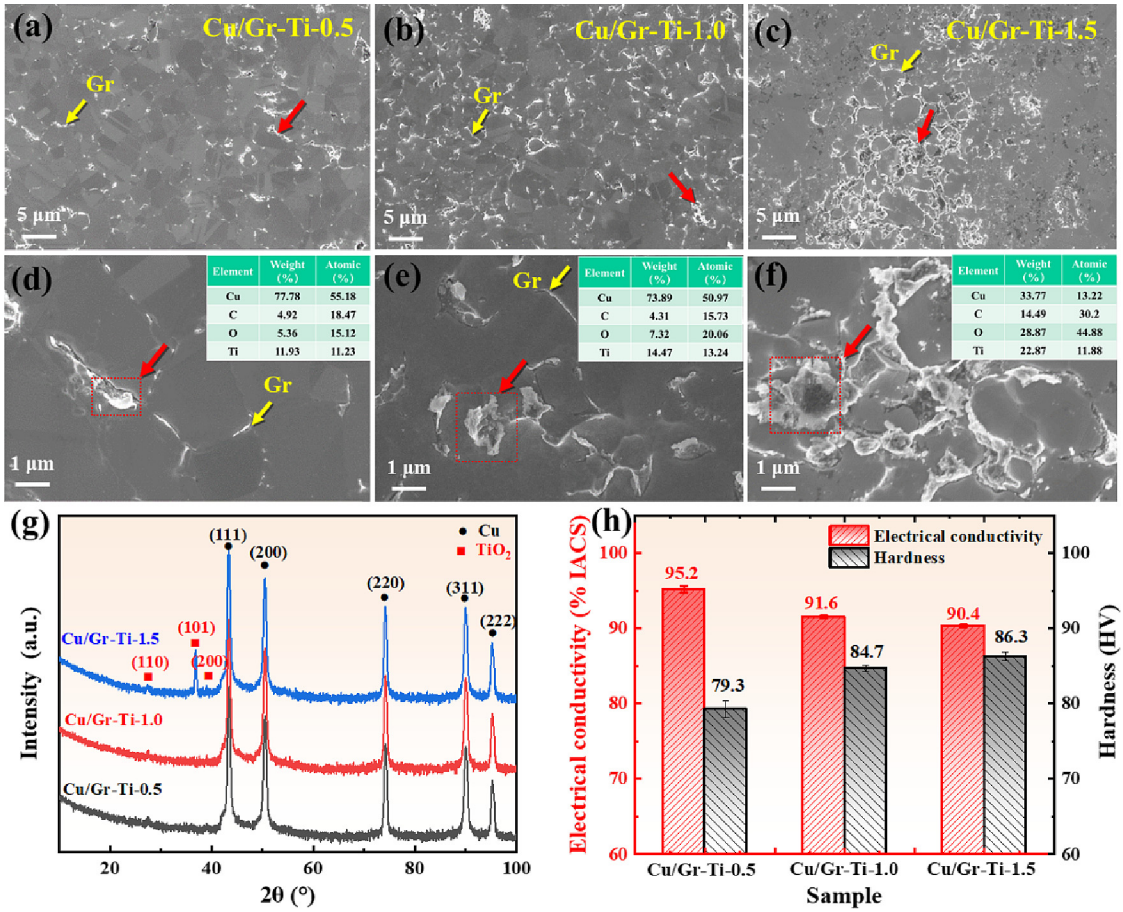

Fig. 6. The microstructures and properties of Cu/Gr-Ti composites as a function of the designed volume fraction of TiO_2: (a), (b), (c) the SEM image of sintered Cu/Gr-Ti composite with the volume percentage of TiO_2 about 0.5%, 1%, and 1.5%, respectively, which is simplified as Cu/Gr-Ti-0.5, Cu/Gr-Ti-1, Cu/Gr-Ti-1.5; (d), (e), (f) the partial enlargement of (a), (b), (c); (g) the XRD pattern; (h) the electrical conductivity and hardness of different sintered Cu/Gr-Ti composites.

3.3. The microstructures and mechanical properties of the cold drawn Cu/Gr-Ti composite wires

The sintered Cu/Gr-Ti composite possesses excellent deformability. It can be directly processed from a sintered cylinder with a diameter of 12.4 mm into a wire with a diameter of 0.49 mm by cold forging, cold rolling, and cold drawing, without internal annealing. The surface of the cold drawn wire is smooth and defect-free, and the internal microstructure is gradually transformed from isotropic equiaxed grains to oriented fibrous grains with the graphene fractured and thinned (Fig. 7). The grain sizes are 0.33 μm in the cross section and up to tens to hundreds of microns in the longitudinal direction. This attributes to the axial tensile stress and radial compressive stress applied to the sample during the cold drawing process.

Fig. 8 presents the microstructure evolution of the Cu/Gr-Ti composite during the cold deformation process. During cold forging [Fig. 8 (a)-(c)], the grains are elongated perpendicular to the forging direction under the radial compressive stress applied. The copper and graphene still maintain a well-bonded interface, without cracks and holes. Bulk TiO_2 particles are still visible in local areas, while TiO_2 nanoparticles can also be found on top of graphene. After cold rolling [Fig. 8(d)-(f)], due to the large deformation, the graphene is fragmented and most aligned discontinuously along the grain boundary, and a small part is embedded in the copper grains, which can hinder dislocation slip between the copper grains, its thickness becomes obviously thinner. Some TiO_2 particles are refined and nailed at the interface. When cold drawing the wire to 0.49 mm, the elongated fibrous grains are clearly visible, and the graphene is further thinned. It is difficult to observe the larger TiO_2 particles. By the high-resolution TEM analysis (HRTEM), TiO_2 particles of 5–10 nm can be found at the interface, which is bonded with Cu matrix and graphene tightly.

Due to this slender fibrous grain structure and strong interfacial bonding, the cold drawn wire exhibits excellent mechanical properties and maintains a high electrical conductivity. Fig. 9(a) gives the room-temperature stress-strain curves of three samples for the cold drawn wire. The uniformity of the sample is very good. Its yield strength and tensile strength can reach 471 MPa and 497 MPa, respectively, which are 21% and 25% higher than those of the pure Cu wire [36], with the electrical conductivity of about 92.1%IACS, for which the content of Ti is only 0.2056 wt% and the graphene is only 0.052 wt%. According to the microstructures, there are several reasons contributing to the superior mechanical properties [23,33,37,38]: (1) the grain refinement caused by the in-situ formed graphene along the grain boundary, which significantly restricts grain growth during sintering, leading to obvious grain refinement strengthening, which can be calculated by the Hall-Petch relationship ($\Delta\sigma_{GR} = \kappa(d_c^{-1/2} - d_m^{-1/2})$, where $\Delta\sigma_{GR}$ is the strengthening contribution from the grain refinement, κ is 0.14 MPa $m^{1/2}$ for Cu, d_c and d_m are the average grain sizes of the Cu/Gr-Ti composite

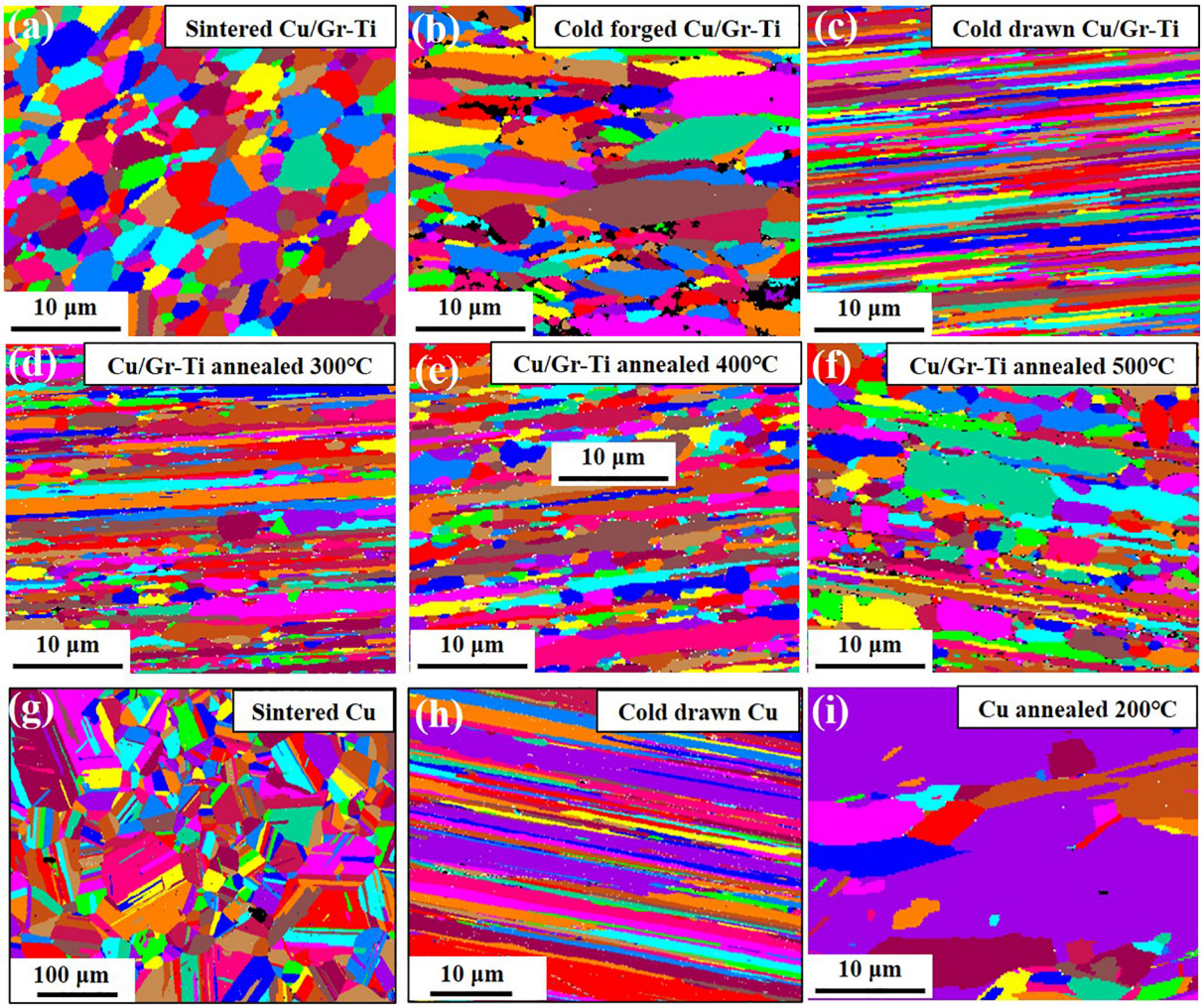

Fig. 7. The EBSD grain maps of the longitudinal section of the Cu/Gr-Ti composites and pure Cu under different processing conditions (a) the sintered sample, (b) the forged sample, (c) the cold drawn wire, (d), (e), (f) the wire annealed at 300 °C, 400 °C and 500 °C for Cu/Gr-Ti; (g) the sintered sample, (h) the cold drawn wire and (i) the wire annealed at 200 °C, 400 °C and 500 °C for pure Cu.

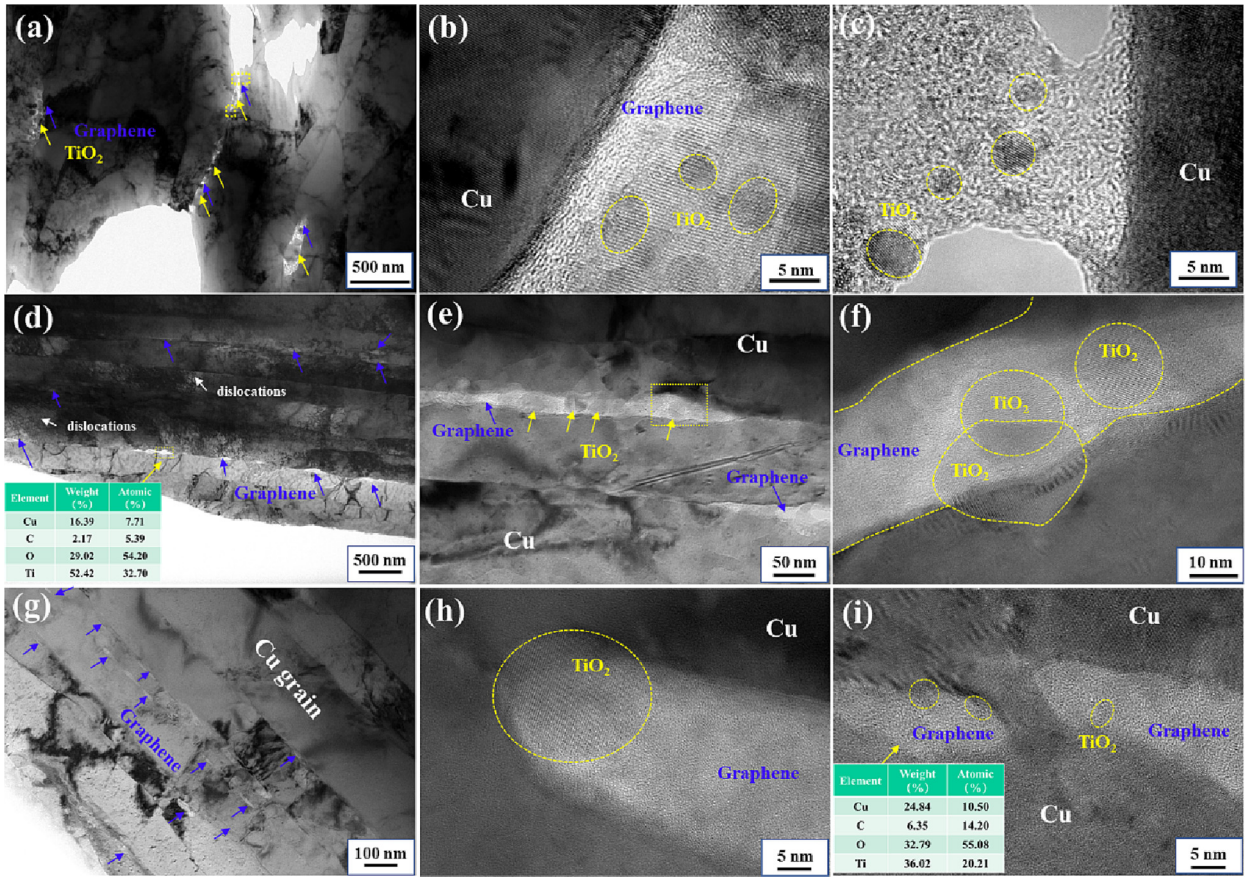

Fig. 8. The TEM images of the Cu/Gr-Ti composite during deformation (a), (b), (c) the cold forged sample; (d), (e), (f) the cold rolled sample; (g), (h), (f) the cold drawn wire; for which (a), (d), (e) and (g) are the bright-field images; (b), (c), (f), (h), and (i) are the HRTEM images of the interface between the Cu-TiO_2-graphene.

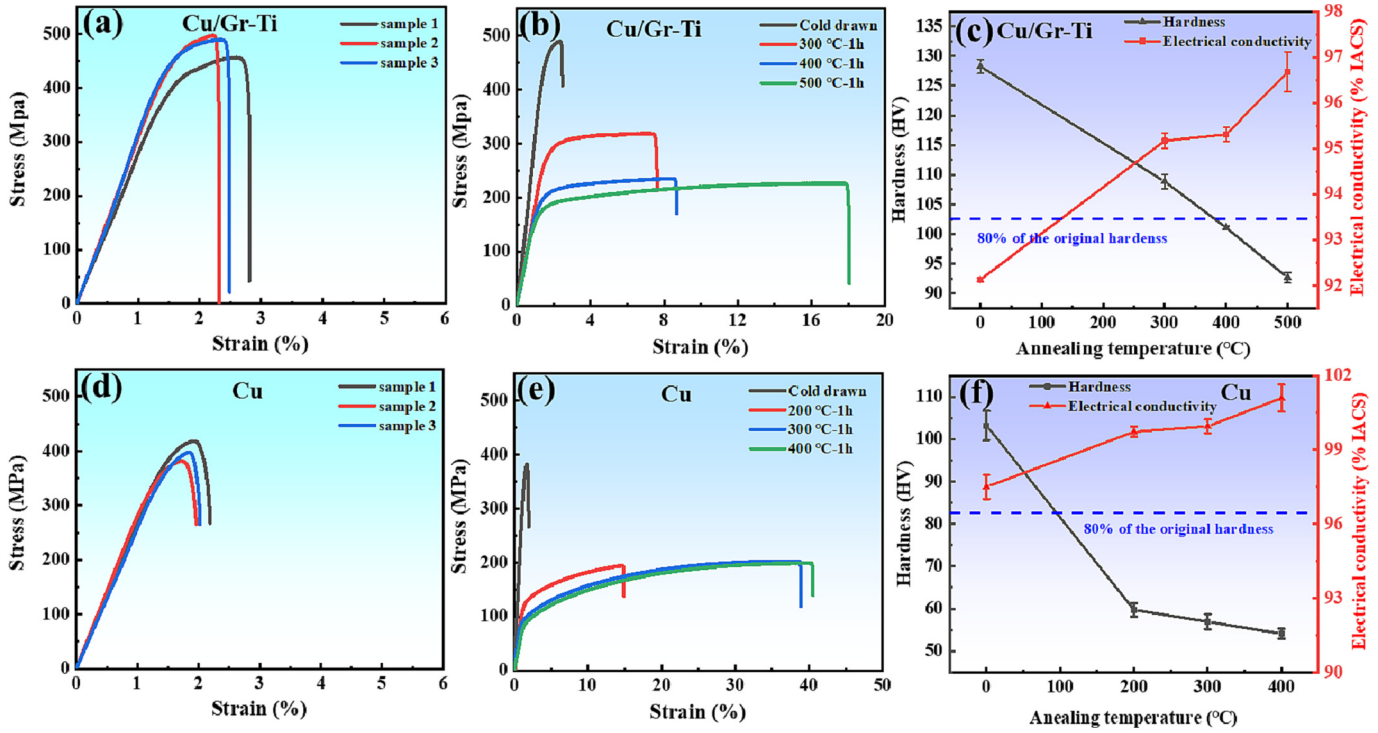

Fig. 9. The room-temperature stress-strain curves of (a) the cold drawn Cu/Gr-Ti composite wire, (b) the annealed Cu/Gr-Ti composite wires at different annealing temperatures, (d) the cold drawn Cu wire and (e) the annealed Cu/Gr-Ti composite wires at different annealing temperatures; (c) and (f) are the variation of hardness and electrical conductivity as a function of the annealing temperature for cold drawn Cu/Gr-Ti composite wire and Cu wire, respectively [36].

and pure Cu, respectively). It is worth noting that, after the cold drawing process, the large deformation further refined the copper grains and the fibrous grains are elongated along the stretching direction. Hence, the strength could be further improved [33]; (2) the tight interfacial bonding brought about by the pinning effect of TiO_2 nanoparticles at the interface and the enhanced mechanical interlocking caused by TiO_2 nanoparticles at the graphene surface achieve a sufficient load transfer between the matrix and the graphene [25,39]; (3) the graphene and TiO_2 nanoparticles obstructed the dislocation movement and caused stress concentrations at the dislocation accumulation sites, leading to dislocation strengthening for which the stress needs to increase when further moving dislocations [23,39]. For the high electrical conductivity, the fibrous grains distributed along the axial direction reduce the scattering of electrons by lateral grain boundaries, the thinned and directionally aligned graphene acts as a channel for electron transport [33].

More importantly, the Cu/Gr-Ti wire also exhibits superior high-temperature performances [Fig. 9(b) and (c)]. After annealing at 300 °C, 400 °C, and 500 °C for 1 h, the yield strength can still be 276 MPa, 187 MPa, and 162 MPa, which is 217%, 122%, and 116% higher than that of a pure Cu under the same annealing condition [Fig. 9(e)]; and the tensile strength maintains 318 MPa, 235 MPa, and 227 MPa. Besides, the elongation increases obviously. The softening temperature, which is always used to study the softening resistance of a material, is defined as the temperature at which the hardness drops to 80% of the initial value after being annealed for 1 h. For the Cu/Gr-Ti wire, its hardness decreases linearly with the annealing temperature, and it is reduced from 128.3 HV to 92 HV when annealing at 500 °C. According to Fig. 9(c), the softening temperature is close to 400 °C, which is much higher than that of pure copper in Fig. 9(f) [18,26]. By carefully observing the grain structures after annealing [Fig. 7(d)-(e)], it is not difficult to find that, recrystallization has begun to occur in local areas when annealing at 300 °C. When further increasing the annealing temperature, the degree of recrystallization continues to increase, and the grains gradually connect and grow up, but still maintaining the original drawn grain orientation. By comparison, the pure Cu wire has been fully recrystallized at 200 °C, and the grains have undergone a secondary growth [Fig. 7(h)-(i)]. Hence, it can be deduced that the presence of graphene and oxides delays the recrystallization, hinders grain boundary migration and grain growth, and makes the composite wire display excellent softening resistance [40]. At the same time, after annealing, some point defects and dislocations inside the wire are eliminated, and the electrical conductivity is improved [18]. This composite wire shows good prospects for high-temperature applications, such as railway contact wire and integrated circuit lead frames.

4. Conclusions

Driven by the idea of in-situ preparation and strengthening through multiphases, we innovatively introduce different organometallic substances, such as aluminum stearate, zinc stearate, and tetrabutyl titanate as the carbon source and nanoparticle formation source to in-situ grows high-quality graphene and oxide nanoparticles in copper through vacuum hot-press sintering. This strategy allows the aggregation and interface-bonding problems of graphene in copper to be solved simultaneously and brings simultaneous high strength, great conductivity, excellent plasticity, and strong softening resistance for TiO_2 doped Cu/graphene composite. The uniformly-distributed 3D graphene network acts as an electron transport channel. The in-situ generated nano-sized TiO_2 particles pin the Cu/graphene interface, hinder the grain growth, and favor load transfer. The TiO_2 and graphene synergistically strengthened Cu composite wire obtained by severe cold deformation exhibits a high electrical conductivity of 92.3% IACS, a high tensile strength of 497 MPa, and a high softening temperature close to 400 °C. And in the future, by selecting more appropriate organometallic substances, adjusting sintering and deformation processes, and regulating the types of nanoparticles and the quality of graphene, Cu/ graphene composite conductors with higher performance can be obtained. The present work provides a good idea for searching for suitable carbon sources to fabricate high-performance Cu-based conductors synergistically improved by in-situ formation of graphene and nanoparticles.

CRediT authorship contribution statement

Tingting Zuo: Conceptualization, Methodology, Formal analysis, Writing – original draft, Writing – review & editing, Funding acquisition. **Meng Wang:** Investigation, Formal analysis. **Jiangli Xue:** Writing – review & editing. **Yadong Ru:** Writing – review & editing. **Yue Wu:** Writing – review & editing. **Fazhu Ding:** Writing – review & editing. **Bo Da:** Writing – review & editing. **Zhuang Xu:** Writing – review & editing. **Peter K. Liaw:** Writing – review & editing. **Zhaoshun Gao:** Conceptualization, Writing – review & editing, Supervision. **Li Han:** Supervision, Writing – review & editing. **Liye Xiao:** Supervision, Writing – review & editing.

Declaration of Competing Interest

The authors declare no competing financial interest.

Data availability

Data will be made available on request.

Acknowledgements

The present work is supported by the National Key Research and Development Program of China [grant number 2021YFB2500600], the Youth Innovation Promotion Association CAS [grant number 2022138], National Natural Science Foundation of China [grant number 51901221], and the Institute of Electrical Engineering, CAS [grant number E155710201 and E155710301]. PKL appreciates the support from the National Science Foundation [grant number DMR-1611180 and 1809640].

References

[1] M. Wang, Y. Jia, Z. Li, M. Guo, Advanced High Strength Conductive Copper Alloy, Central South University Press, Changsha, 2015.
[2] S.J. Kim, D.H. Shin, Y.S. Choi, H. Rho, M. Park, B.J. Moon, Y. Kim, S. Lee, D.S. Lee, D.S. Lee, T. Kim, S.H. Lee, K.S. Kim, B.H. Hong, S. Bae, Ultrastrong graphene-copper core-shell wires for high-performance electrical cables, ACS Nano 12 (2018) 2803, https://doi.org/10.1021/acsnano.8b00043.
[3] L. Lu, Y. Shen, X. Chen, L. Qian, K. Lu, Ultrahigh strength and high electrical conductivity in copper, Science 304 (2004) 422, https://doi.org/10.1126/science.1092905.
[4] L.X. Sun, N.R. Tao, K. Lu, A high strength and high electrical conductivity bulk CuCrZr alloy with nanotwins, Scr. Mater. 99 (2015) 73–76, https://doi.org/10.1016/j.scriptamat.2014.11.032.
[5] W.A.D.M. Jayathilaka, A. Chinnappan, S. Ramakrishna, A review of properties influencing the conductivity of CNT/Cu composites and their applications in wearable/flexible electronics, J. Mater. Chem. C 5 (2017) 9209, https://doi.org/10.1039/c7tc02965a.
[6] M. Bakir, I. Jasiuk, Novel metal-carbon nanomaterials: a review on covetics, Adv. Mater. Lett. 8 (2017) 884, https://doi.org/10.5185/amlett.2017.1598.
[7] C. Subramaniam, T. Yamada, K. Kobashi, A. Sekiguchi, D.N. Futaba, M. Yumura, K. Hata, One hundred fold increase in current carrying capacity in a carbon nanotube-copper composite, Nat. Commun. 4 (2013) 2202, https://doi.org/10.1038/ncomms3202.
[8] I.A. Kinloch, J. Suhr, J. Lou, R.J. Young, P.M. Ajayan, Composites with carbon nanotubes and graphene: an outlook, Science 362 (2018) 547, https://doi.org/10.1126/science.aat7439.
[9] L. Xiong, K. Liu, J. Shuai, Z. Hou, L. Zhu, W. Li, Toward high strength and high electrical conductivity in super-aligned carbon nanotubes reinforced copper, Adv. Eng. Mater. 20 (2018) 1700805, https://doi.org/10.1002/adem.201700805.
[10] O. Hjortstam, P. Isberg, S. Söderholm, H. Dai, Can we achieve ultra-low resistivity in carbon nanotube-based metal composites, Appl. Phys. A Mater. Sci. Process. 78 (2004) 1175, https://doi.org/10.1007/s00339-003-2424-x.
[11] Z. Yang, J. Tian, Z. Yin, C. Cui, W. Qian, F. Wei, Carbon nanotube- and graphene-based nanomaterials and applications in high-voltage supercapacitor: a review, Carbon 141 (2019) 467, https://doi.org/10.1016/j.carbon.2018.10.010.

[12] J. Baringhaus, M. Ruan, F. Edler, A. Tejeda, M. Sicot, A. Taleb-Ibrahimi, A. Li, Z. Jiang, E.H. Conrad, C. Berger, C. Tegenkamp, W.A. de Heer, Exceptional ballistic transport in epitaxial graphene nanoribbons, Nature 506 (2014) 349–354, https://doi.org/10.1038/nature12952.
[13] P. Hidalgo-Manrique, X. Lei, R. Xu, M. Zhou, I.A. Kinloch, R.J. Young, Copper/graphene composites: a review, J. Mater. Sci. 54 (2019) 12236, https://doi.org/10.1007/s10853-019-03703-5.
[14] K. Chu, J. Wang, Y.P. Liu, Z.R. Geng, Graphene defect engineering for optimizing the interface and mechanical properties of graphene/copper composites, Carbon 140 (2018) 112, https://doi.org/10.1016/j.carbon.2018.08.004.
[15] H. Yue, L. Yao, X. Gao, S. Zhang, E. Guo, H. Zhang, X. Lin, B. Wang, Effect of ball-milling and graphene contents on the mechanical properties and fracture mechanisms of graphene nanosheets reinforced copper matrix composites, J. Alloys Compd. 691 (2017) 755, https://doi.org/10.1016/j.jallcom.2016.08.303.
[16] R.T. Mathew, S. Singam, P. Kollu, S. Bohm, M.J.N.V. Prasad, Achieving exceptional tensile strength in electrodeposited copper through grain refinement and reinforcement effect by co-deposition of few layered graphene, J. Alloys Compd. 840 (2020), 155725, https://doi.org/10.1016/j.jallcom.2020.155725.
[17] X. Zhang, Y. Xu, M. Wang, E. Liu, N. Zhao, C. Shi, D. Lin, F. Zhu, C. He, A powder-metallurgy-based strategy toward three-dimensional graphene-like network for reinforcing copper matrix composites, Nat. Commun. 11 (2020) 2775, https://doi.org/10.1038/s41467-020-16490-4.
[18] Z. Gao, T. Zuo, M. Wang, L. Zhang, B. Da, Y. Ru, J. Xue, Y. Wu, L. Han, L. Xiao, In-situ graphene enhanced copper wire: a novel electrical material with simultaneously high electrical conductivity and high strength, Carbon 186 (2022) 303, https://doi.org/10.1016/j.carbon.2021.10.015.
[19] J. Hwang, T. Yoon, S.H. Jin, J. Lee, T.S. Kim, S.H. Hong, S. Jeon, Enhanced mechanical properties of graphene/copper nanocomposites using a molecular-level mixing process, Adv. Mater. 25 (2013) 6724, https://doi.org/10.1016/j.compositesb.2020.108088.
[20] Z. Dong, Y. Peng, Z. Tan, G. Fan, Q. Guo, Z. Li, D. Xiong, Simultaneously enhanced electrical conductivity and strength in Cu/graphene/Cu sandwiched nanofilm, Scr. Mater. 187 (2020) 296, https://doi.org/10.1016/j.scriptamat.2020.06.051.
[21] X. Zhang, C. Shi, E. Liu, F. He, L. Ma, Q. Li, J. Li, W. Bacsa, N. Zhao, C. He, Achieving high strength and high ductility in metal matrix composites reinforced with a discontinuous three-dimensional graphene-like network, Nanoscale 9 (2017) 11929, https://doi.org/10.1039/c6nr07335b.
[22] Q. Xiao, X. Yi, B. Jiang, Z. Qin, J. Hu, Y. Jiang, H. Liu, B. Wang, D. Yi, In-situ synthesis of graphene on surface of copper powder by rotary CVD and its application in fabrication of reinforced cu-matrix composites, Adv. Mater. Sci. 2 (2017) 1, https://doi.org/10.1016/j.jallcom.2020.155182.
[23] Z. Xu, X. Zhang, N. Zhao, C. He, Synergistic strengthening effect of in-situ synthesized WC_{1-x} nanoparticles and graphene nanosheets in copper matrix composites, Comp. Part A 133 (2020), 105891, https://doi.org/10.1016/j.compositesa.2020.105891.
[24] M. Yang, L. Weng, H. Zhu, F. Zhang, T. Fan, D. Zhang, Leaf-like carbon nanotube-graphene nanoribbon hybrid reinforcements for enhanced load transfer in copper matrix composites, Scr. Mater. 138 (2017) 17, https://doi.org/10.1016/j.scriptamat.2017.05.024.
[25] S. Guo, X. Zhang, C. Shi, D. Zhao, E. Liu, C. He, N. Zhao, Comprehensive performance regulation of Cu matrix composites with graphene nanoplatelets in situ encapsulated Al_2O_3 nanoparticles as reinforcement, Carbon 188 (2022) 81, https://doi.org/10.1016/j.carbon.2021.11.054.
[26] M. Wang, T. Zuo, J. Xue, Y. Ru, Y. Wu, Z. Xu, Z. Gao, L. Han, L. Xiao, A novel approach for in-situ preparation of copper/graphene composite with high hardness and high electrical conductivity, Mater. Lett. 319 (2022), 132219, https://doi.org/10.1016/j.matlet.2022.132219.
[27] M.P. Lavin-Lopez, J.L. Valverde, M.I. Ruiz-Enrique, L. Sanchez-Silva, A. Romero, Thickness control of graphene deposited over polycrystalline nickel, New J. Chem. 39 (2015) 4414, https://doi.org/10.1039/C5NJ00073D.
[28] Y. Jin, B. Hu, Z. Wei, Z. Luo, D. Wei, Y. Xi, Y. Zhang, Y. Liu, Roles of H2 in annealing and growth times of graphene CVD synthesis over copper foil, J. Mater. Chem. A 2 (2014) 16208, https://doi.org/10.1039/C4TA02557A.
[29] D. Yang, A. Velamakanni, G. Bozoklu, S. Park, M. Stoller, R.D. Piner, S. Stankovich, I. Jung, D.A. Field, C.A. Ventrice, R.S. Ruoff, Chemical analysis of graphene oxide films after heat and chemical treatments by X-ray photoelectron and Micro-Raman spectroscopy, Carbon 47 (2009) 145, https://doi.org/10.1016/j.carbon.2008.09.045.
[30] Y. Zhang, W. Wu, K. Zhang, C. Liu, A. Yu, M. Peng, J. Zhai, Raman study of 2D anatase TiO2 nanosheets, Phys. Chem. Chem. Phys. 18 (2016) 32178–32184, https://doi.org/10.1039/C6CP05496J.
[31] S.K. Islam, J.R. Lombardi, Raman enhancement (SERS) of the surface phonon modes of TiO_2, Chem. Phys. Lett. 806 (2022), 140040, https://doi.org/10.1016/j.cplett.2022.140040.
[32] R. Jiang, X. Zhou, Q. Fang, Z. Liu, Copper-graphene bulk composites with homogeneous graphene dispersion and enhanced mechanical properties, Mater. Sci. Eng. A 654 (2016) 124, https://doi.org/10.1016/j.msea.2015.12.039.
[33] T. Li, Y. Wang, M. Yang, H. Hou, S. Wu, High strength and conductivity copper/graphene composites prepared by severe plastic deformation of graphene coated copper powder, Mater. Sci. Eng. A 826 (2021), 141983, https://doi.org/10.1016/j.msea.2021.141983.
[34] Z. Chen, W. Ren, L. Gao, B. Liu, S. Pei, H.M. Cheng, Three-dimensional flexible and conductive interconnected graphene networks grown by chemical vapour deposition, Nat. Mater. 10 (2011) 424, https://doi.org/10.1038/nmat3001.
[35] X. Liu, F. Wang, W. Wang, H. Wu, Interfacial strengthening and self-healing effect in graphene-copper nanolayered composites under shear deformation, Carbon 107 (2016) 680, https://doi.org/10.1016/j.carbon.2016.06.071.
[36] T. Zuo, M. Wang, J. Xue, Y. Ru, L. Zhang, B. Da, Y. Wu, Z. Xu, Z. Gao, P.K. Liaw, L. Han, L. Xiao, Superior electrical conductivity-strength combination of an in-situ fabricated La_2O_3-doped copper/graphene composite conductor, Carbon 197 (2022) 455, https://doi.org/10.1016/j.carbon.2022.06.086.
[37] S.E. Shin, H.J. Choi, J.Y. Hwang, D.H. Bae, Strengthening behavior of carbon/metal nanocomposites, Sci. Rep. 5 (2015) 16114, https://doi.org/10.1038/srep16114.
[38] Y. Yang, M. Liu, S. Zhou, W. Ren, Q. Zhou, W. Zhang, Strengthening behaviour of continuous graphene network in metal matrix composites, Carbon 182 (2021) 825, https://doi.org/10.1016/j.carbon.2021.06.067.
[39] S. Guo, X. Zhang, C. Shi, E. Liu, C. He, F. He, N. Zhao, Enhanced mechanical properties and electrical conductivity of graphene nanoplatelets/cu composites by in situ formation of Mo_2C nanoparticles, Mater. Sci. Eng. A 766 (2019), 138365, https://doi.org/10.1016/j.msea.2019.138365.
[40] X. Guo, Z. Xiao, W. Qiu, Z. Li, Z. Zhao, X. Wang, Y. Jiang, Microstructure and properties of Cu-Cr-Nb alloy with high strength, high electrical conductivity and good softening resistance performance at elevated temperature, Mater. Sci. Eng. A 749 (2019) 281, https://doi.org/10.1016/j.msea.2019.02.036.